

Optimum Hollowness of Normally Loaded Rings

Subodh Subedi and Deje-Kossu Zahai

Abstract—Advancements in manufacturing and material technology has redefined the approach of design for machine components. Additive manufacturing processes have enabled designers to manufacture for design and functionality. With Design for Additive Manufacturing (DfAM) approach, components can be manufactured with holes in them, including rolling contact components. These hollow components save material, weight, have shorter manufacturing lead times and possibly a higher rolling contact fatigue resistance. Hollowness is defined as the volume percentage of intentional void in load carrying member. Finite element analysis is performed to obtain compressive and tensile stresses on rings and square plates with centric holes in them. The values obtained, are then plotted against the distance from center and hollowness. Observations from numerical analysis are further confirmed with experimental results using strain gages. The results show a moderate increase in strain up to about 20% to 35% hollowness depending on the type of specimen and loading in both finite element and experimental results. Beyond these values, which represent the optimum hollowness, the strains increase along a steep curve. The above results form a basis to examine the effect of hollowness for rolling contact machine elements for their fatigue life. RCF life of solid and hollow discs are examined using theoretical analysis, finite element tools and experiments. The results indicate that some hollow load bearing machine components with enhanced RCF life can be fabricated, leveraging recent advances in Additive Manufacturing.

Index Terms— Stresses and strains in Rings, Normal Loading, Optimum Hollowness.

1 INTRODUCTION

MACHINES have been in use to human help for centuries now. Discovery of wheel can be taken as the first step in building the first machine, humans ever built. Today, almost every human activity is assisted by a machine, directly or indirectly. Various components in a machine work together to provide an intended output. Each component has its own function and is designed for a specific purpose. A good component design satisfies all the functional requirements by using best suited material, optimum weight, size, shape and product life. Traditional manufacturing processes involve more than one-step to modify the existing stocks to obtain a final product. For example, to manufacture a simple cylindrical shaft, a round stock is taken and then reduced to the required dimension by cutting, turning and facing. Manufacturing of components such as gears, bearings, cams etc., that require complex geometrical, mechanical and metallurgical properties involve lot more steps, time, energy and cost. With the advancements in material science and manufacturing technology, improvements in design have significantly reduced the size and weight of machines. Bulkier engines have become compact with higher power, efficiency, and sophistication. Tasks that required heavy machines can now be accomplished with lighter and smaller but better efficient machines. 3D printing has saved time in product research and development, making it possible to try out different permutations and combinations of design variables to achieve the best output in shortest possible time, effort, material consumption and costs. Apart from their use for rapid prototyping in the last 30 years, they have been used in rapid manufacturing as well [1]. Obvious benefits of this technology are reduction of life cycle, material mass, energy, scrap and harmful auxiliary processes etc. One major advantage of Additive Manufacturing (AM) is that it has redefined the approach of product design and development. This technology has enabled designers to choose 'manufacturing the design' vs. 'design for manufacturing'

approach [2]. Designers are no longer constrained by manufacturing processes and have the liberty to create and manufacture parts that would be more efficient and better at their functionality across all industries including aerospace, biomedical and automotive.

Hollow components such as hollow gears, bearings, cams etc., which were unimaginable, can now be easily designed and manufactured to required precision. They have larger surface areas, allowing lubricants to dissipate more heat from the bodies. In addition, if AM printed, these hollow components could be saving time and cost as well. Though they might not be stronger than their solid counterparts, the benefits of their ability to flex could be used to possibly extend the fatigue life under rolling contact

Not much of an investigation has been done regarding the stress field variation with hollowness of machine components. Circular rings have been studied in greater depths to find the tensile strength of brittle materials such as concrete and rock using a widely known technique called Brazilian Disc test as shown in Figure 1. Brazilian Disc test is an indirect testing method where tensile strength of rocks is determined by the stresses at failure of rings loaded in uniaxial diametric compression. For the normally loaded disk, stresses induced are compressive and tensile along the loading axis and the axis normal to that, respectively. The tensile stress is almost constant near the center of the disk under compression. It is assumed that failure occurs at the point of maximum tensile stress, i.e. at the center of the disc [3], [4]. Equation (1) is used to calculate the maximum tensile stress σ_T using the Brazilian Disc test.

$$\sigma_T = \frac{2P}{\pi Dw} = 0.636 \frac{P}{Dw} \quad (1)$$

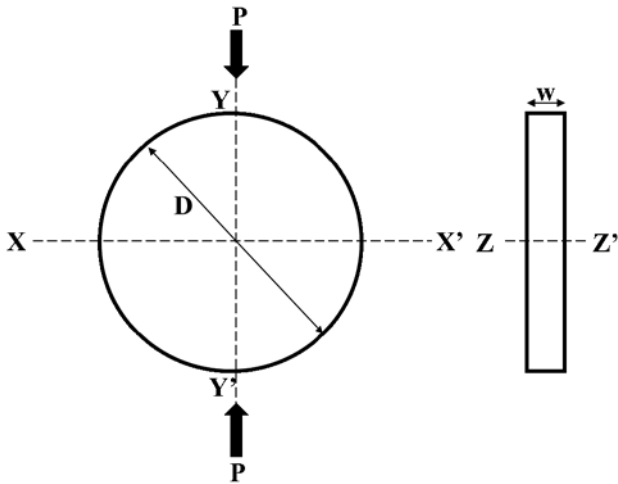


Fig. 1. Schematics of Brazilian Disc Test

No specific focus on stress variation with change in size of holes or hollowness were found in literature except for the test for failure of rock samples in Brazilian disc test, thus, all the reference made herein are based on the same. The procedure and results of Brazilian Disc test can be related with the work described in this document as it assumes that even rocks are homogenous, isotropic and linearly elastic before brittle failure occurs [5]. Initiation of crack is considered as a failure criteria and most of the study has been focused on defining the failure criteria based on the location of crack initiation site. Yanagidani et al. [6], Chen et al. [7] have shown that the crack initiation site would be located at the center of the Brazilian disc based on the Griffith fracture criterion. Fairhurst [8], Hooper [9], Hudson et al. [10], Swab et al. [11] have shown that the crack initiation points are located away from the center of the discs. Yanagidani et al. [5] first made use of strain gages to study the stress field on rock samples. Filon (1924) came up with the methods of calculating stresses in rings that are point loaded on the inside boundary [12]. Stress field on a diametrically compressed circular disc was discussed by Timoshenko in 1951. His results for total stress distribution in hollow rings of unit thickness were based on two assumptions: (1) The surface remains plane and the normal stresses over the cross section is hyperbolic. (2) The total stresses are distributed linearly. The results from his work based on these assumptions were good for the stresses along X-axis but gave significant error in predicting the stress along Y-axis for rings [13].

Most of these studies have been used to examine the stress on hollow components or to determine the tensile yield strength of rock samples as in the case of Brazilian Disc Test [3], [4]. Hobbs was skeptical of the results of the test as he observed multiple wedge shaped fractures from close to the loading platens, leading to prior tensile failure along the loaded diameter [5]. To avoid the stress concentration at the disk-jaw interface, he proposed the use of a circular disc with a small central hole. He studied the effect of the size of hole in

the stress variation within these specimens and came up with the following equations to determine stress on the discs with holes. The stresses in a ring loaded diametrically are given by (2), (3) and (4).

$$\sigma_{rr} = \frac{1}{r^2} \frac{\partial^2(X)}{\partial \theta^2} + \frac{1}{r} \frac{\partial(X)}{\partial r} \tag{2}$$

$$\sigma_{r\theta} = -\frac{\partial}{\partial r} \frac{1}{r} \frac{\partial(X)}{\partial \theta} \tag{3}$$

$$\sigma_{\theta\theta} = \frac{\partial^2}{\partial r^2}(X) \tag{4}$$

Where X is the stress function assumed by Filon [20]. r is defined as $R_i > r > R_o$ where R_i is the inside radius and R_o is the outside radius of the ring. σ_{rr} is the radial stress, θ is the angle from the horizontal axis along which stress is being measured, $\sigma_{\theta\theta}$ is the hoop stress, and $\sigma_{r\theta}$ is the shear stress. For a disk as shown in Figure 2, with central hole radius R_i , external radius R_o , thickness w being compressed along the vertical diameter with a load of P , the maximum tensile stress σ_T along $\theta = \pm \frac{\pi}{2}$ and maximum compressive stress σ_c at $\theta = 0$ and π are approximately given by,

$$\sigma_T = \frac{P}{\pi D_o w} (6 + 38q^2) \tag{5}$$

$$\sigma_c = \frac{P}{\pi D_o w} (10 + 10q^2) \tag{6}$$

where q is the ratio of internal to external radius [5]. Kourkoulis and Markides [14] concluded that the stress field strongly depends on the kind of externally imposed load that influences the results, when inner radius approaches the outer one.

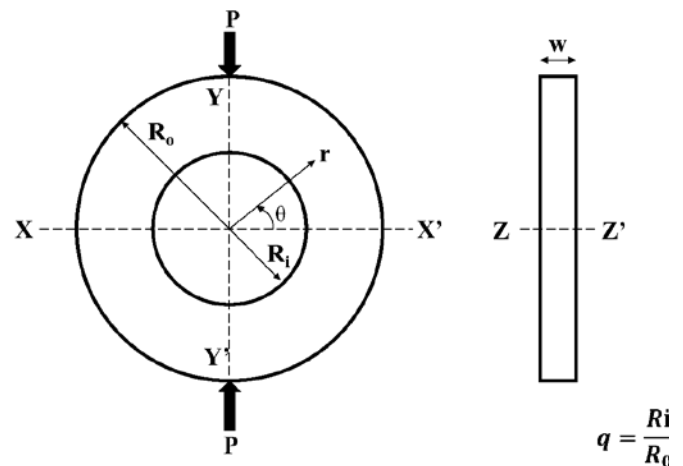


Fig. 2. Ring under Normal Diametric Compressive Loading

2 HOLLOWNESS OF COMPONENTS

Load bearing components such as gears, shafts, bearings are critical components in machine design. A precise selection of size, material, mass and shape is necessary for proper functioning and utmost efficiency. Hollow components are obviously lighter and susceptible to collapse under different loading conditions. These components on the other hand, could possibly minimize inertial mass, reduce material consumption, increase power efficiency and durability, and provide larger surface areas for cooling. Hollowness has mostly been defined for cylindrical roller bearing as the ratio of inside diameter to outside diameter. Researchers have defined optimum hollowness for these cylindrical hollow bearings that have maximum rolling contact fatigue failure lives. Darji and Vadkharia [15] have defined optimum hollowness for cylindrical rolling element of bearings based on finite element simulation for minimum contact stress and longest fatigue life under normal loads. They have found that fatigue life for the cylindrical bearings under normal load is maximum in between 60% to 70% hollowness. This corresponds to 36% to 49% hollowness in terms of volume ratio of intentional void to the total volume. Jadayil et al. [16] compared the fatigue lives of solid and hollow rollers in pure rolling contact, where rollers were subjected to combined normal and tangential loads. It was found that due to flexibility of hollow cylinders, contact stresses are redistributed, peak stress is decreased and thus fatigue life is maximum at around 60% hollowness. Beyond these values the cylinders become too flexible and compromise their load bearing capacity.

The objective of the work presented here is to examine the effect of hollowness in machine components and define the optimum hollowness of these components as well as Rolling contact components under fatigue loading.

One of the current constrains in part of Design for Manufacture and Assembly (DfMA) approach is that, it hardly supports the manufacture of hollow components to be used instead of solid machine components. Lack of machining ability and insufficient data about the use of hollow machine components, make their use very rare. Load bearing components such as bearings, gears, shafts, cams, wheels could be manufactured with hollow cores and used, if only, their response in terms of functionality and reliability were further studied.

Studies have shown that hollow components are better than their solid counterparts, especially in the case of handling contact stresses. Hollow components can flex under normal compressive loading and thus better distribute contact stresses [15], [16].

The problem is to identify the possible relation between stress and hollowness on any machine component and then define an optimum hollowness for the component based on its ability to perform its functions satisfactorily. Optimum hollowness is the maximum hollowness that any component can have and still satisfy its functional requirements as compared to their solid counterparts. The judgement for optimum is relative and needs a careful investigation of the distribution of

stress field on a defined cross section. Since AM components have comparable strength and are at par with the conventionally manufactured components, hollow AM components can be used instead of solid ones. If so, what could be the maximum hollowness that these components can have?

3 HOLLOWNESS INVESTIGATION

To investigate the effect of hollowness on different specimens, finite element analysis is performed using ANSYS Workbench®. Wang et al. [17] carried out stress analysis on a flattened Brazilian disc specimen, using ANSYS® but, their intent was to determine the elastic modulus, tensile strength, and fracture toughness for brittle rocks. In this paper, our focus is on finding the effect of hollowness on stresses and strains for rings under compressive loads.

3.1 Finite Elements Models

Finite element models are created in ANSYS®. Normal Stresses and deformation along X and Y axes for 4 types of models were then studied in detail. These models Figure 3, can be categorized based on the loading or the shape of the void. For a concentrated loading, the load is applied on circular specimens where the top plate and bottom plate make a line contact along the z-axis, meaning, there is a line of contact between each of the loading plate and the circular specimens. Distributed loading is used for square Specimens compressed using flat plates.

Shape of voids is also used to categorize the models such as concentric regular where the specimens have identical shape voids in them as their outer shape. Concentric irregular shapes are obtained where the voids in the specimens have different shapes than their outer shapes.

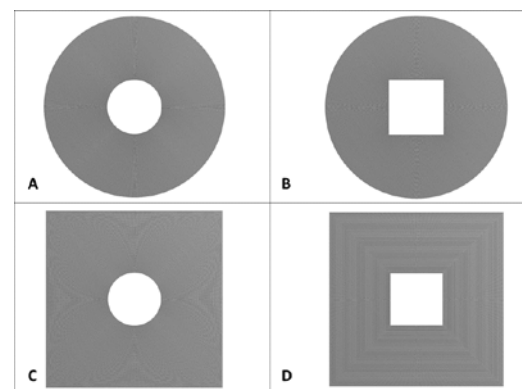


Fig. 3. Different Categories of Specimens

The finite element models were validated using the analytical results from Hobbs' investigation of stress in rings [13]. Figure 4 shows a comparison between analytical results and maximum stress along two perpendicular axes in the finite element model for circular specimen with circular holes. Maximum compressive and tensile stress values along loading axis and axis perpendicular to that are compared to the maximum compressive and maximum tensile stress obtained

from (5) and (6). As evident from the two plots, the stresses along the axes follow the similar pattern, as do the stresses from the equations. In the figure, the blue lines represent the maximum compressive stress and the red lines the maximum tensile stress. Figure 4(A) shows results from Hobb while Figure 4(B) represents from the FE analysis.

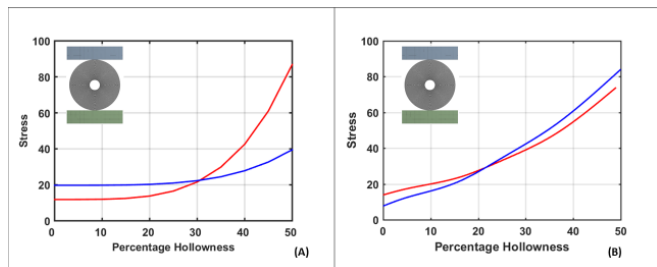


Fig. 4. Maximum Stress Variation with Hollownes.

After running the solution, the results were obtained for stress, strain, and deformations. Two paths were created along the Y and X axes from the outer edge of each model to the center of the models. Equivalent stress, equivalent strain, normal stress, normal strain, total deformation and directional deformation along these two paths were obtained and the values were analyzed.

3.2 Finite Elements Results

Results from the FEA of hollow circular disc and square plates are presented herein. Stress and strain values are extracted along the vertical loading axis and the horizontal axis.

3.2.1 Stress Variation along Axes

Figure 5 to Figure 7 show variation of different type of stresses along the two axes due to hollowness in the circular specimens. The stresses are plotted against hollowness percentages in these normally loaded aluminum models. Y is the loading axis whereas X is the horizontal axis. The plots indicate that all types of stresses increase steeply beyond 40% hollowness, meaning the chances of failure is very high beyond 40% hollowness. Thus, the investigation for optimum hollowness is focused on specimens below 40 % hollowness.

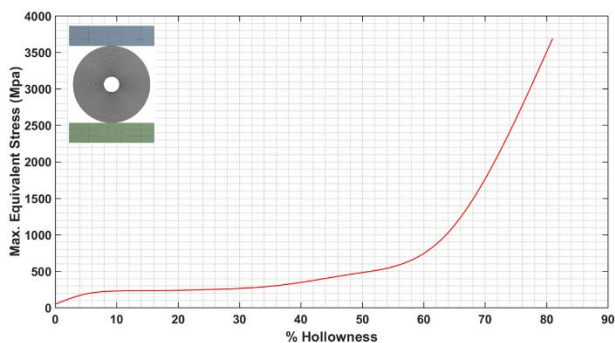


Fig. 5. Maximum Equivalent Stress Variation with Percentage Hollowness.

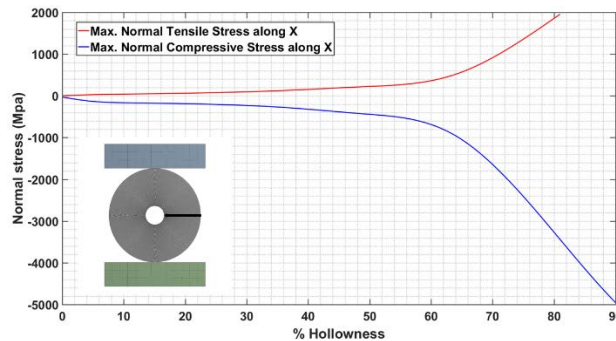


Fig. 6. Maximum Normal Stress variation with Hollowness along X-axis.

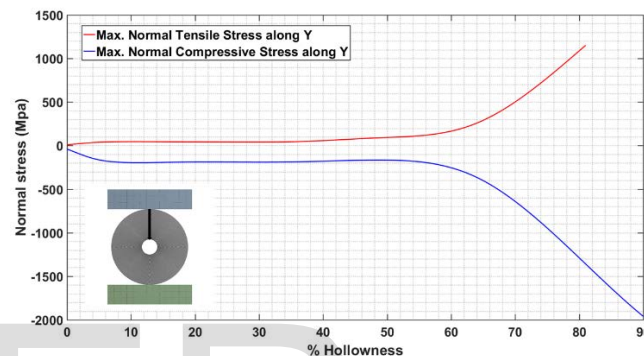


Fig. 7. Maximum Normal Stress variation with Hollowness along Y-axis.

3.2.2 Stress and deformation variation along Axes

Stress and deformation values were analyzed for all four type of specimens shown in Figure 3. All of specimens were compressed with 10kN load along the Y-axis. Stress and deformation values along the Y-axis and X-axis were recorded and plotted against the distance from outside edge to inside edge. For circular specimen with circular holes, Figure 8 to Figure 11 show stress and deformation variation. The results can be summarized as follows: (1) Normal stress along Y is maximum for specimens with solid specimens (0% Hollowness). It is initially compressive, then it rises, goes tensile almost near the inside edge and then drops to zero for all specimens of different hollowness. As the bending stresses get dominant on the inside edges, stress on the 49% hollow specimen changes to tensile. (2) Normal stress along X is maximum for 49% hollowness specimen. The stress is tensile for the solid specimen whereas for other specimens, it is compressive, reaches the peak and then bounces back to zero at the inside edge. (3) Maximum deformation along X and Y are both experienced for 49% hollow specimens. The deformation values are almost constant along both the axes. Results presented in the figure were also obtained for other type of specimen but will not be reported or discussed up herein.

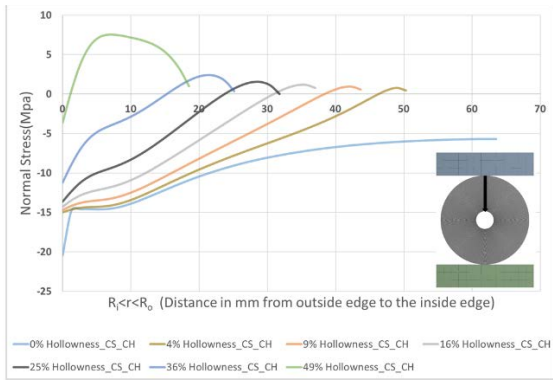


Fig. 8. Normal Stress Variation along Y

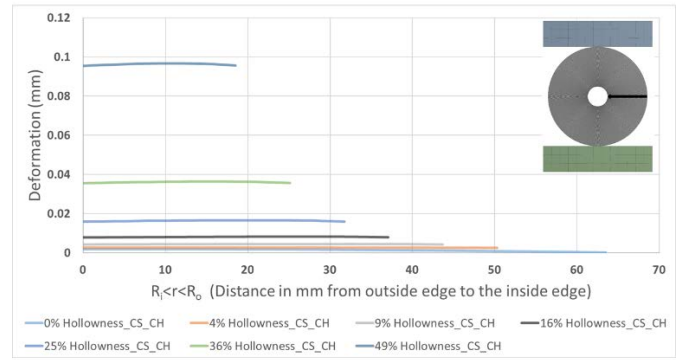


Fig. 11. Directional Deformation Variation along X-axis

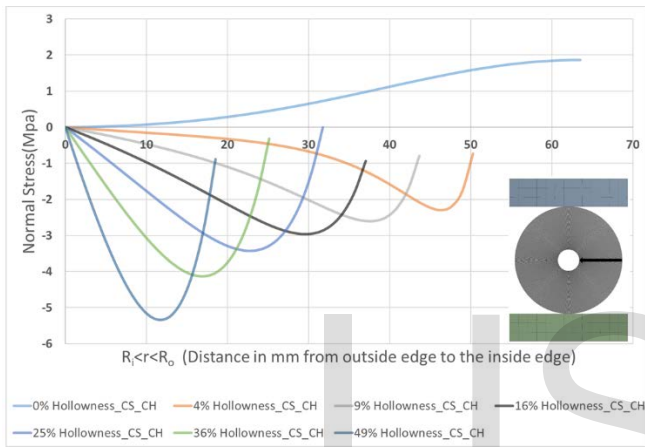


Fig. 9. Normal Stress Variation along X-axis.

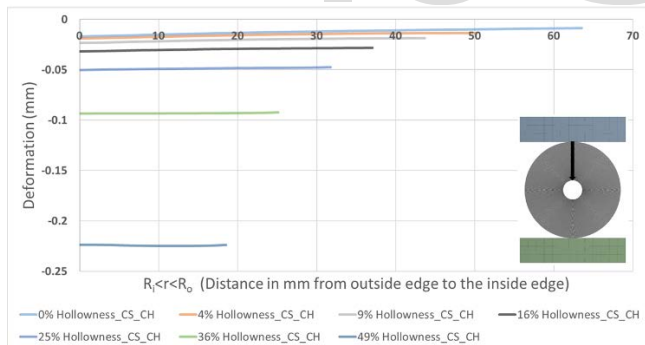


Fig. 10. Directional Deformation Variation along Y-axis

3.2.3 Strain Variation along Axes

Figure 12 shows the location of measurement of normal strain along the loading axis (Y-axis) and the axis perpendicular to that (X-axis). Figure 13 and 14 show the variation of strain for the change in load on Circular specimens with circular holes and square specimen with circular hole measured at different point along X and Y-axes.

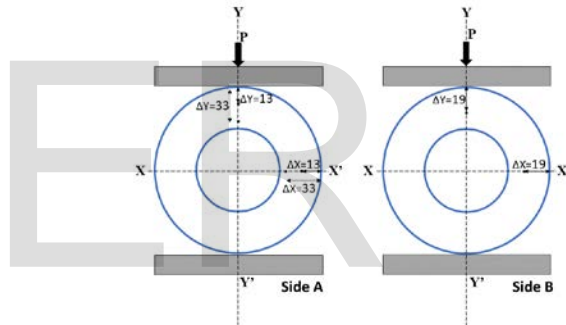


Fig. 12. Strain Measurement Points on Circular Specimens with Circular Holes

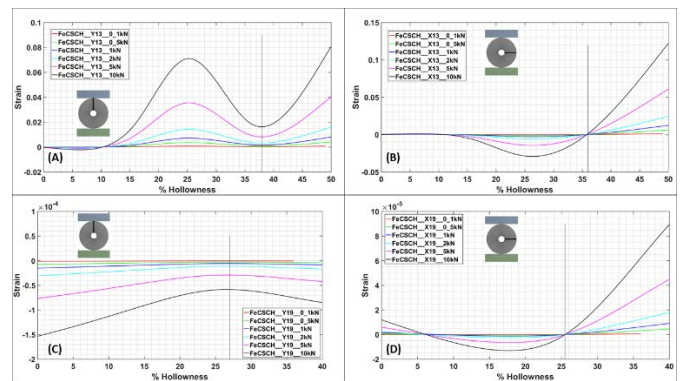


Fig. 13. Strain Variation at $\Delta X=13\text{mm}$ on Circular Specimens with Circular Holes

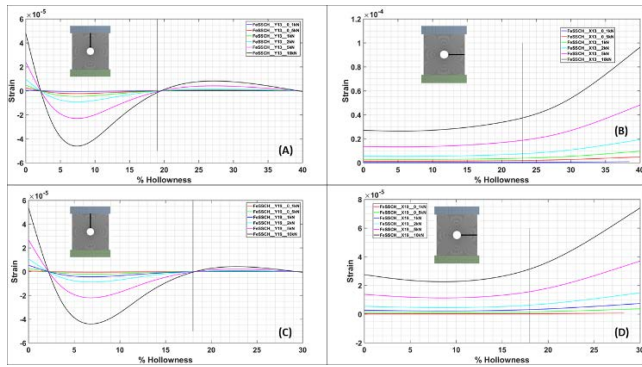


Fig. 14. Strain Variation at $\Delta Y=13\text{mm}$ on Square Specimens with Circular Holes.

Figure 13 shows the variation of normal strain variation at different locations within the specimen for increase in hollowness percentage. Finite element results show that normal strain rises steeply after about 40% hollowness. Optimum hollowness for this loading and specimen case varies between 25% to 40%. Strain rises significantly beyond the optimum hollowness values, indicating higher chances of failure in the specimens.

Figure 14 shows the variation of normal strain variation at different locations within the specimen for increase in hollowness percentage. Finite element results show that optimum hollowness for this loading case is around 20% as strain rises significantly beyond 20% hollowness along Y and X-axis.

4 CONCLUSION

Square and circular rings normally loaded have been investigated. Based on the proposed definition of hollowness, rings from 0 to 50% hollowness were loaded in compression. The load created compressive and tension loads in the components. Using theoretical and finite element analysis, it was shown that these members could have up to 40% hollowness without drastically reducing their load carrying capability. This is a preliminary investigation to determine the amount and the location of voids in machine components to avoid failure. Future study will address this issue along with the fatigue life investigation. However, the results presented here indicate that some load carrying or transmitting machine components can be fabricated with measurable voids leveraging recent advances in Additive Manufacturing.

REFERENCES

[1] Diegel O., Singammani S., Reay S., Withell A., (2010), "Tools for Sustainable Product Design: Additive Manufacturing, Journal of Sustainable Development", vol.3No. 3: September 2010.

[2] Esmaeilian B., Behdad S., Wang B., 2016, "The evolution and future of manufacturing: A review", Journal of Manufacturing Systems 39(2016)79-100.

[3] ISRM (1978), "Suggested Methods for Determining Tensile Strength of Rock Materials", Int J Rock Mech Min Sci Geomech Abstr 15(3):99-103. doi:10.1016/0148-9062(78)90003-7.

[4] ASTM (2008) D 3967-08, "Standard Test Method for Splitting Tensile Strength of Intact Rock Core Specimens", ASTM International, West Conshohocken, USA.

[5] Hobbs D.W., (1965), "An Assessment of a Technique for Determining the Tensile Strength of Rock", Brit. J. Appl. Phys. 1965, Vol.16.

[6] Yanagidani T., Sano O., Terada M., and Ito I., (1978), "The observation of cracks propagating in diametrically-compressed rock discs", Intl J Rock Mech Min Sci Geomech Abstr, 15(5), 225-235.

[7] Chen S, Yue ZQ, Tham LG, "Digital Image-based Numerical Modeling Method for Prediction of Inhomogeneous Rock Failure", Int J Rock Mech Min Sci 41(6):939-957.

[8] Fairhurst C. (1964), "On the Validity of the 'Brazilian' Test for Brittle Materials", Int J Rock Mech Min Sci Geomech Abstr 1(4): 535-546. doi: 10.1520/GTJ103134.

[9] Hooper JA. (1971), "The Failure of Glass Cylinders in Diametral Compression", J Mech Phys Solids 19(4):179-200.

[10] Hudson JA. (1969), "Tensile strength and Ring Test", Int J Rock Mech Min Sci Geomech Abstr 6(1):91-97. doi:10.1016/0148-9062(69)90029-1.

[11] Swab JJ., Yu J., Gamble R., Kilczewski S., (2011), "Analysis of the Diametral Compression Method for Determining the Tensile Strength of Transparent Magnesium Aluminate Spinel", Int J Fract. doi: 10.1007/s10704-011-9655-1.

[12] Filon L.N.G., (1924) "The Stresses in a Circular Ring, Selected Engineering Papers", The Institution of Civil Engineers, London.

[13] Timoshenko SP., Goodier JN., "Theory of Elasticity". 2nd ed. New York: McGraw Hill, 1951.

[14] Kourkoulis S.K., Markides Ch.F., (2014), "Stresses and Displacements in a Circular Ring Under Parabolic Diametral Compression", International journal of Rock Mechanics and Mining Sciences 71 (2014) 272-292.

[16] Darji P.H., Vadkharla D.P., (2008), "Determination of Optimum Hollowness for Hollow Cylindrical Rolling Element Bearing", Proceeding of IMECE 2008, October 31-Nov. 6, 2008 MA, USA.

[16] Abu Jadayil W., Flugard D., Qamhiyah A., "Fatigue Life Investigation of Solid and Hollow Rollers in Pure Rolling Contact", Proceedings of WTC2005, World Tribology Congress III, Sept.12-16, 2005, Washington D.C, USA.

[17] Want et al. (2004), "The Flattened Brazilian Disc Specimen used for Testing Elastic Modulus, Tensile Strength and Fracture Toughness of Brittle Rocks: Analytical and Numerical Results", Int J Rock Mech Min Sci 41(2):245-253.